

AN OVERVIEW OF STATE-OF-THE-ART DENOISING AND DEMOSAICKING TECHNIQUES: TOWARD A UNIFIED FRAMEWORK FOR HANDLING ARTIFACTS DURING IMAGE RECONSTRUCTION

Bart Goossens*, Hiep Luong, Jan Aelterman, Aleksandra Pižurica and Wilfried Philips

Ghent University - TELIN - IPI - iMinds
Sint-Pietersnieuwstraat 41, B-9000 Ghent, Belgium
bart.goossens@telin.ugent.be

ABSTRACT

Pushing the physical limits of the camera sensors brings significant challenges to image post-processing techniques, which often have to work under various constraints, such as low-power, limited memory and computational resources. Other platforms, e.g., desktop PCs suffer less from these issues, allowing extra room for improved reconstruction. Moreover, the captured images are subject to many sources of imperfection (e.g., noise, blur, saturation) which complicate the processing. In this paper, we give an overview of some recent work aimed at overcoming these problems. We focus especially on denoising, deblurring and demosaicking techniques.

I. INTRODUCTION

In the past decade, there has been a significant increase in diversity of both display devices and image acquisition devices, going from tiny cameras in mobile phones to 100 megapixel (MP) digital cameras. The number of megapixels of digital camera sensors steadily increases while the sensor elements become smaller and smaller. Consequently, more sophisticated image post-processing techniques are required to solve the problems caused by noise [1]. In general, there is a tendency to push the physical limits of acquisition, resulting in larger digital images with more noise (both from the sensors and analog-to-digital converters in the camera), blur and a large variety of other artifacts. On the other hand, there is a big diversity in platforms (mobile devices, tablets, desktop PCs, ...), displays and cameras. Due to restrictions in computational resources, limited memory and batteries, a compromising solution consists of integrating relatively simple post-processing/reconstruction schemes into the cameras. On other platforms, more computational resources and more memory may be available, so that full frame buffers can be processed, potentially giving extra room for image enhancement and improved reconstruction. Many cameras, especially the more expensive single-lens-reflex cameras, allow storing the images in a raw format onto the camera's SSD memory card. Then the user can reconstruct the images on a desktop PC using RawTherapee,¹ Adobe(R) Lightroom(TM) or related software packages.

Another issue is that applying demosaicking and denoising sequentially often lead to a poor image quality due to incorrect interpolation of color intensities and noise [1] (and idem for other artifact corrections). Recently, more sophisticated

*Bart Goossens acknowledges support by a postdoctoral fellowship of the Research Foundation - Flanders (FWO, Belgium).

¹<http://rawtherapee.com>

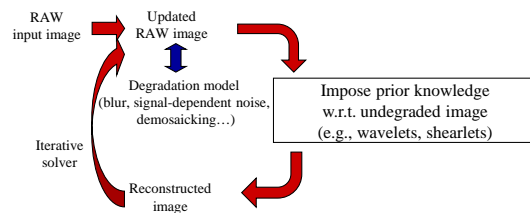


Fig. 1. A unified reconstruction framework.

techniques have been developed that jointly solve several degradations (e.g., noise, demosaicking, blur, saturation) at once, using the mathematical framework of estimation theory, leading to much better reconstruction results. Several notable examples are: *joint denoising and demosaicking* [1]–[4], *joint demosaicking and deconvolution* [5]–[8], *high dynamic range reconstruction and denoising* [9], [10] and *declipping and denoising* [11].

In this paper, we will give an overview of some of these novel developments in Section II. Next, we present a unified reconstruction framework for dealing with several degradations simultaneously. In this framework (see Figure 1), the degradation is naturally modeled in the image domain, while the image model is defined in a multi-resolution transform domain (e.g., wavelets, curvelets, shearlets, ...). In the image model, *sparsity* (which states that the image can be represented using a small number of coefficients with significant magnitude) plays an important role. This decoupling has the important consequence that a reconstruction technique can be designed by:

- 1) Selecting an appropriate multiresolution transform (based on image content and/or computational resource, power and memory considerations) and sparsity measure (Section III-A).
- 2) Incorporating a realistic camera noise model (Section III-B).
- 3) Using a “generic” solver to reconstruct the image (Subsection III-C).

Despite the generality of this approach, due to the iterative nature of the solver, the algorithms are computationally intensive and are best suited for the desktop PC platform (e.g., reconstructing a 10MP may take several seconds using a GPU). However, for certain combinations of degradations (such as demosaicking+denoising), several simplifications can be made, which often lead to non-iterative solutions that could be implemented in the camera hardware.

II. A BRIEF OVERVIEW OF DENOISING AND DEMOSAICKING TECHNIQUES

II-A. Image denoising

Well-known image denoising techniques include total variation [12], bilateral filtering [13] and anisotropic diffusion (e.g. [14], [15]). Nonlinear diffusion schemes [16] compute solutions of a set of coupled partial differential equations (PDEs) that are inspired by heat-diffusion equations. For the restoration of blurred images with *Poisson noise*, the Richardson-Lucy (RL) method has been proposed in [17]. Because RL does not include regularization, extensions include RL with Tikhonov-Miller regularization [18] and RL with TV regularization [18].

The NLMeans filter [19] exploits non-local similarity of image patches (e.g., bricks in a wall). By its success, many improvements have been proposed (e.g. [20]–[22]). In a related technique, BM3D [23], similar patches are grouped in a 3D stack and subsequently denoised in the 3D transform domain, resulting in very appealing visual results. Very recently, some methods have emerged that combine NLMeans/BM3D ideas with dictionary learning.

With the advent of wavelets, wavelet shrinkage has attracted the interest of many researchers, due to its simplicity and effectiveness. In wavelet transform decompositions of images with white noise, high-pass subbands mainly consist of noisy coefficients with occasionally large magnitudes caused by edges and textures. Shrinkage techniques reduce the magnitude of the non-significant coefficients (coefficients with a magnitude that is smaller than a given threshold) to suppress noise. Several techniques have then been specifically developed to optimize the thresholds in terms of a well-chosen criterion [24].

Sophisticated image priors/distributions help to improve wavelet-based denoising methods: Bayesian estimators exploit the statistical properties of wavelet coefficients, together with the good time-frequency localization properties of the wavelets. Some techniques use univariate priors (e.g., [25], [26]) while other methods also exploit the local correlations of the wavelet coefficients (e.g., [27], [28]).

II-B. Joint image demosaicking+denoising

Due to price and power consumption reasons, the use of color filter arrays (CFAs), such as the Bayer CFA is still very popular. In [29], a broad overview of image demosaicking techniques can be found. While in the past, demosaicking and denoising have mostly been performed sequentially, more recently *joint* demosaicking and denoising (sometimes called *denoisaicing* [2]) have been developed [1], [2], [4], [30].

Similar to image denoising, wavelet-based demosaicking has been explored by Hirakawa in [31]. Simple linear demosaicking rules can be derived to de-modulate or de-multiplex the chrominance and luminance information in the wavelet domain. When a wavelet-transform is available in hardware, the joint demosaicking and denoising can be performed very efficiently and at a low computational cost in this transform domain. The main limitation is a hard assumption for the chrominance and luminance bandwidths. These assumptions are often invalid for real-world images, resulting in color and zipper artifacts. In recent work [32], we have extended the approach of Hirakawa to the complex wavelet domain and by integrating local spatial adaptivity in the algorithm. Because of

these innovations, it becomes possible to alleviate the problems with the bandwidth assumptions. In [3] we have extended this technique to denoising+demosaicking by integrating a Bayesian Gaussian Scale Mixture prior.

II-C. Joint image demosaicking+deblurring+denoising

Also, joint demosaicking and deblurring have been studied by various researchers [5]–[8]. Blur is caused by the camera capturing a scene that is out-of-focus, or due to the presence of fast motion (motion blur). Because the human visual system is more sensitive to sudden luminance changes than to color changes, it often suffices to deblur only the luminance components. For example, in [5], the luminance component is first estimated and then deblurred. Then, a fast demosaicking algorithm is used to reconstruct the chrominance components. Finally, the deblurred luminance component and the blurred chrominance components are combined. Paliy et al. focus on removing Poisson noise using LPA-ICI (Local Polynomial Approximation - Intersections of Confidence Intervals) [6]. Soulez and Thiébaud developed a Bayesian restoration technique using edge-preserving spatial and spectral regularization [7].

III. A UNIFIED RECONSTRUCTION FRAMEWORK

III-A. Multiresolution Image Models

Using multiresolution transforms, images can be approximated by successively adding detail information to a coarse (low-pass) layer in subsequent refinement steps. This approach is effective as natural images are often low-pass in nature. The *wavelet transform* offers a compromise between spatial and frequency localization of image features. The classical wavelet transform, while ideally suited for one-dimensional signals, turns out to be sub-optimal for representing images, because the transform can not adapt well to the image geometry. Some improved multidirectional transforms are steerable pyramids [33], dual-tree complex wavelets [34], curvelets [35] and shearlets [36]. Shearlets have the main advantage of allowing a very fine directional analysis with an arbitrary number of directions per scale. Furthermore, shearlets are well suited for representing data defined on a Cartesian grid. In particular, this opens a number of possibilities to reduce the redundancy, computation and memory requirements of the transform [37]. We therefore choose shearlets for the results in this paper.

III-B. Noise model

Accurate noise modeling is crucial for good reconstruction quality. In [10], we have presented a noise model that incorporates electronic, photon and fixed pattern noise, and several post-processing steps in the camera. The main idea is that after every processing step, the statistical properties of the noise can be calculated based on the processing function. In particular, a Taylor approximation with one or two terms can be used to accurately determine the noise bias and variance. In particular, we have the measured exposure value x_i at position i :

$$x_i \sim \mathcal{P}(E_i \Delta t) \quad \text{and} \quad z_i = f(\sqrt{\alpha} x_i) \quad (1)$$

where the scene irradiance E_i is integrated over a time Δt and where the pixel value z_i is obtained by applying the camera response function (CRF) to $\sqrt{\alpha} x_i$, where $\sqrt{\alpha}$ is a gain factor. The CRF models several nonlinear operations in

the digital camera, such as gamma correction, ISO setting, white balancing, contrast enhancement and quantization, and is camera/manufacturer dependent. Working with the Poisson distribution in combination with the nonlinear CRF is not practical in general, therefore, we use a Poissonian-Gaussian approximation similar to [38]. The idea is to express the statistical moments of z_i as a function of those of E_i . This yields [10]:

$$E[z_i|E_i] \approx \zeta(E_i, 0) + \frac{1}{2} \frac{\partial^2 \zeta}{\partial \nu^2} \Big|_{\nu=0} \quad \text{and} \quad \text{Var}[z_i|E_i] \approx \frac{\partial \zeta}{\partial \nu} \Big|_{\nu=0}, \quad (2)$$

with

$$\zeta(E, \nu) = f \left(E \Delta t + \nu \sqrt{\sigma_o^2 + \alpha \Delta t E + \beta (\Delta t E)^2} \right) \quad (3)$$

where σ_o^2 is an offset noise term and where β is the gain fixed pattern noise parameter. The three parameters σ_o^2 , α and β can easily be determined by performing local noise variance analysis in a setup, in which multiple (at least two) low dynamic range images with different exposure times are acquired [10]. The result is that for every pixel in the image, the noise variance of this pixel can be accurately estimated.

III-C. Reconstruction algorithm

Under the Poissonian-Gaussian approximation, a linear degradation caused by the CFA, blur and additive noise is given by the following matrix-vector formulation:

$$\vec{z} = \vec{A} \vec{B} \vec{y} + \vec{v} \quad (4)$$

where $\vec{z} = [z_i, i = 1, \dots, n] \in \mathbb{R}^n$ (with n the number of pixels of the sensor), $\vec{y} \in \mathbb{R}^{3n}$ and $\vec{v} \in \mathbb{R}^n$ is a Gaussian noise term, with statistical moments as in (2). The matrix $\vec{B} \in \mathbb{R}^{n \times 3n}$ represents the blur operator and $\vec{A} \in \mathbb{R}^{n \times 3n}$ denotes the Bayer downsampling operator. To solve the ill-posed inverse problem, the following cost function can be minimized:

$$\hat{\vec{y}} = \arg \min_{\vec{y}} \frac{\lambda}{2} \left\| \vec{C} (\vec{A} \vec{B} \vec{y} - \vec{z}) \right\|_2^2 + \left\| (\vec{D} \otimes \vec{S}) \vec{y} \right\|_p^p, \quad (5)$$

where λ is a regularization parameter, \otimes denotes the Kronecker product, \vec{C} is a diagonal matrix with the reciprocal of the noise variances $1/\text{Var}[z_i|E_i]$ on its diagonal. \vec{S} is a spatially sparsifying transform (see Subsection III-A) that operates on each color channel separately. $\vec{D} \in \mathbb{R}^{3 \times 3}$ is a color decorrelation matrix. $\|\cdot\|_p = (\sum_i \|f_i\|^p)^{1/p}$ is the ℓ_p -norm. The cost function (5) can then be minimized using convex optimization methods, such as split-Bregman [39], split augmented Lagrangian or primal-dual methods [8]. Finally, traditional camera corrections (color correction, white balancing, gamma) are applied to the obtained solution $\hat{\vec{y}}$. In principle, these non-linear corrections can also be incorporated in (4), but due to the non-convexity of the resulting cost function, this poses extra challenges, which forms the topic of our current research.

IV. RESULTS

We evaluate the reconstruction algorithm from Subsection III-C on a RAW digital camera image, captured with a Nikon D60 camera with 55-200mm lens at exposure time 1/640s, aperture f/6.3 and ISO 100. Visual results are given in Figure 2 for the AMaZE algorithm (RawTherapee) and our method. In our method, denoising, deblurring and demosaicing cooperate and compensate each other's deficiencies. This leads to sharp



(a)



(b)

Fig. 2. Reconstruction results (a) RawTherapy - AMaZE demosaicking (b) Joint demosaicking & deblurring.

images with reduced noise while at the same time demosaicing color artifacts suppressed.

V. CONCLUSION

Several improvements in reconstruction quality of raw data from digital cameras are obtained by solving several sub-problems (e.g., denoising, demosaicking, deblurring, ...) jointly rather than sequentially. This generic technique is especially promising because several other linear or even non-linear effects can be incorporated in the reconstruction model (such as image sensor deficiencies, high dynamic range, ...). The study of these extensions is the topic of our currently ongoing research.

VI. REFERENCES

- [1] K. Hirakawa, *Single-Sensor Imaging: Methods and Applications for Digital Cameras*. CRC Press, 2008, ch. Color Filter Array Image Analysis for Joint Denoising and Demosaicking.

- [2] L. Condat, "A simple, fast and efficient approach to denoising: Joint demosaicking and denoising," in *Proc. 17th IEEE Int. Conf. Image Processing (ICIP)*, Hong Kong, China, 2010, pp. 905–908.
- [3] B. Goossens, J. Aelterman, H. Luong, A. Pižurica, and W. Philips, "Complex wavelet joint denoising and demosaicking using gaussian scale mixtures," in *IEEE Int. Conf. Image Processing*, Melbourne, Australia, Sept. 15–18 2013, pp. 445–448.
- [4] P. Chatterjee, N. Joshi, K. S. B., and Y. Matsushita, "Noise suppression in low-light images through joint denoising and demosaicking," in *Proc. IEEE Conf. Computer Vision and Pattern Recognition (CVPR)*, 2011, pp. 321–328.
- [5] S. Har-Noy, S. Chang, and T. Nguyen, "Demosaicking images with motion blur," in *Proc. of IEEE Int. Conf. Acoustics, Speech and Sig. Proc. (ICASSP)*, 2010, pp. 1006–1009.
- [6] D. Paliy, A. Foi, R. Bilcu, V. Katkovnik, and K. Egiazarian, "Joint deblurring and demosaicking of Poissonian Bayer-data based on local adaptivity," in *Proc. European Sig. Proc. conf. (EUSIPCO)*, 2008.
- [7] F. Soulez and E. Thiebaut, "Joint deconvolution and demosaicking," in *Proc. IEEE Int. Conf. Image Proc.*, 2009, pp. 145–148.
- [8] H. Luong, B. Goossens, J. Aelterman, A. Pižurica, and W. Philips, "A Primal-Dual Algorithm for Joint Demosaicking and Deconvolution," in *IEEE Int. Conf. Image Processing (ICIP2012)*, Orlando, Florida, USA, Sep. 30 - Oct. 3 2012, pp. 2801–2804.
- [9] B. Goossens, H. Luong, J. Aelterman, A. Pižurica, and W. Philips, "Reconstruction of High Dynamic Range Images with Poisson Noise Modeling and Integrated Denoising," in *IEEE Int. Conf. Image Processing (ICIP2011)*, Brussels, Belgium, Sept. 11–14 2011, pp. 3429–3432, accepted.
- [10] —, "Realistic Camera Noise Modeling with Application to Improved HDR Synthesis," *EURASIP Journal on Advances in Signal Processing*, 2012.
- [11] A. Foi, "Practical denoising of clipped or overexposed noisy images," in *Proc. 16th European Signal Process. Conf. (EUSIPCO)*, Lausanne, Switzerland, 2008.
- [12] L. Rudin and S. Osher, "Total variation based image restoration with free local constraints," in *Proc. of IEEE International Conference on Image Processing (ICIP)*, vol. 1, nov 1994, pp. 31–35.
- [13] C. Tomasi and R. Manduchi, "Bilateral filtering for gray and color images," *International Conference on Computer Vision (ICCV)*, pp. 839–846, 1998.
- [14] L. I. Rudin, S. Osher, and E. Fatami, "Nonlinear total variation based noise removal algorithms," *Physica D*, vol. 60, pp. 259–268, November 1992.
- [15] T. F. Chan, S. Osher, and J. Shen, "The digital tv filter and nonlinear denoising," *IEEE Trans. Image Processing*, vol. 10, no. 2, pp. 231–241, February 2001.
- [16] J. Weickert, *Anisotropic Diffusion in Image Processing*, ser. ECMI Series. Teubner-Verlag, 1998.
- [17] W. H. Richardson, "Bayesian-based iterative method of image restoration," *Journal of the Optical Society of America*, vol. 62, no. 1, pp. 55–59, January 1972.
- [18] N. Dey, L. Blanc-Féraud, C. Zimmer, P. Roux, Z. Kam, J. Olivo-Marin, and J. Zerubia, "3D microscopy deconvolution using richardson-lucy algorithm with total variation regularization," July 2004, research Report 5272, INRIA.
- [19] A. Buades., B. Coll., and J. Morel, "A non local algorithm for image denoising," *SIAM interdisciplinary journal: Multiscale Modeling and Simulation*, vol. 2, no. 2, pp. 60–65, 2005.
- [20] M. Mahmoudi and G. Sapiro, "Fast image and video denoising via nonlocal means of similar neighborhoods," *IEEE Signal Processing Letters*, vol. 12, no. 12, pp. 839–842, dec 2005.
- [21] C. Kervrann, J. Boulanger, and P. Coupé, "Bayesian Non-Local Means Filter, Image Redundancy and Adaptive Dictionaries for Noise Removal," in *Proc. Int. Conf. on Scale Space and Variational Methods in Computer Visions (SSVM'07)*, Ischia, Italy, 2007, pp. 520–532.
- [22] B. Goossens, H. Luong, A. Pižurica, and W. Philips, "An improved Non-Local Means Algorithm for Image Denoising," in *2008 International Workshop on Local and Non-Local Approximation in Image Processing*, Ghent, Belgium, dec 2008, (invited paper).
- [23] K. Dabov, A. Foi, V. Katkovnik, and K. Egiazarian, "Image denoising by sparse 3d transform-domain collaborative filtering," *IEEE Transactions on image processing*, vol. 16, no. 8, pp. 2080–2095, 2007.
- [24] D. L. Donoho, "De-noising by soft-thresholding," *IEEE Trans. Inform. Theory*, vol. 41, no. 3, pp. 613–627, May 1995.
- [25] E. P. Simoncelli and E. H. Adelson, "Noise removal via Bayesian wavelet coring," in *Proc. IEEE Internat. Conf. Image Proc. ICIP*, Lausanne, Switzerland, 1996.
- [26] M. S. Crouse, R. D. Nowak, and R. G. Baranuik, "Wavelet-based statistical signal processing using hidden Markov models," *IEEE Trans. Signal Proc.*, vol. 46, no. 4, pp. 886–902, "April" 1998.
- [27] L. Şendur and I. Selesnick, "Bivariate shrinkage with local variance estimation," *IEEE Signal Processing Letters*, vol. 9, no. 12, pp. 438–441, Dec 2002.
- [28] J. Portilla, V. Strela, M. Wainwright, and E. Simoncelli, "Image denoising using scale mixtures of gaussians in the wavelet domain," *IEEE Trans. on image processing*, vol. 12, no. 11, pp. 1338–1351, Nov. 2003.
- [29] B. Gunturk, J. Glotzbach, Y. Altunbasak, R. Schaffer, and R. Mersereau, "Demosaicing: color filter array interpolation," *IEEE Sig. Proc. Magazine*, vol. 22, no. 1, pp. 44–54, 2005.
- [30] K. Hirakawa and T. W. Parks, "Joint demosaicing and denoising," *IEEE Trans. Image Process.*, vol. 15, no. 8, pp. 2146–2157, aug 2006.
- [31] K. Hirakawa, X.-L. Meng, and P. J. Wolfe, "A framework for wavelet-based analysis and processing of color filter array images with applications to denoising and demosaicing," *IEEE Int. Conf. Acoust. Speech Signal Process. (ICASSP 2007)*, pp. 597–600, Apr. 2007.
- [32] J. Aelterman, B. Goossens, A. Pižurica, and W. Philips, "Fast, locally adaptive demosaicing of color filter array images using the dual-tree complex wavelet packet transform," *Plos One*, vol. 9, no. 6, pp. e98937 (1–16), 2014.
- [33] E. Simoncelli, W. T. Freeman, E. H. Adelson, and D. J. Heeger, "Shiftable Multi-scale Transforms," *IEEE Trans. Information Theory*, vol. 38, no. 2, pp. 587–607, 1992.
- [34] I. W. Selesnick, R. G. Baraniuk, and N. G. Kingsbury, "The Dual-Tree Complex Wavelet Transform," *IEEE Signal Processing Magazine*, vol. 22, no. 6, pp. 123–151, nov 2005.
- [35] E. Candès, L. Demanet, D. Donoho, and L. Ying, "Fast Discrete Curvelet Transforms," *Multiscale modeling and simulation*, vol. 5, no. 3, pp. 861–899, 2006.
- [36] G. Kutyniok and D. Labate, "Construction of Regular and Irregular Shearlets," *J. Wavelet Theory and Appl.*, vol. 1, pp. 1–10, 2007.
- [37] B. Goossens, J. Aelterman, H. Luong, A. Pižurica, and W. Philips, "Design of a Tight Frame of 2D Shearlets Based on a Fast Non-iterative Analysis and Synthesis algorithm," in *IEEE Optics & Photonics 2011, Wavelets and Sparsity XIV*, San Diego, CA, USA, Aug. 21–25 2011, p. p. 81381Q, invited paper.
- [38] A. Foi, M. Trimeche, V. Katkovnik, and K. Egiazarian, "Practical Poissonian-Gaussian noise modeling and fitting for single-image raw-data," *IEEE Trans. image Process.*, vol. 17, no. 10, pp. 1737–1754, Oct. 2008.
- [39] T. Goldstein and S. Osher, "The split Bregman method for L1 regularized problems," *Computational and Applied Math*, University of California, Tech. Rep. 08–29, 2008.